Journal of Hazardous Materials 262 (2013) 887–895

Contents lists available at ScienceDirect

Journal of Hazardous Materials

journal homepage: www.elsevier.com/locate/jhazmat

Origin, mobility, and temporal evolution of arsenic from a low-contamination catchment in Alpine crystalline rocks

Eric Pili[a,b,*], Delphine Tisserand[c], Sarah Bureau[c]

[a] CEA, DAM, DIF, F-91297 Arpajon, France
[b] Institut de Physique du Globe de Paris-Sorbonne Paris Cité, CNRS, Université Paris Diderot, 1 rue Jussieu, F-75238 Paris cedex 05, France
[c] Institut des Sciences de la Terre (ISTerre) Université Joseph Fourier and CNRS, BP 53, 38041 Grenoble cedex 9, France

HIGHLIGHTS

- $\delta^{34}S_{SO4}$ vs. [As] and $\delta^{18}O_{SO4}$ vs. As^{V}/As^{III} correlations provide new tools even for low [As].
- Long-term and high-resolution monitoring shows droughts enhance pyrite dissolution.
- Major effect of 2003 European heatwave on pyrite dissolution and [As] increase.

ARTICLE INFO

Article history:
Received 16 December 2011
Received in revised form 1 May 2012
Accepted 2 July 2012
Available online 7 July 2012

Keywords:
Arsenic
Pyrite
Sulfate
Isotopes
Monitoring

ABSTRACT

The reduction to 10 μg/l of the limit for arsenic in drinking water led many resource managers to deal with expensive treatments. In the very common case of arsenic levels close to the recommended maximum concentration, knowing the origin and temporal evolution of As has become of great importance. Here we present a case study from an alpine basin. Arsenic speciation, isotopic compositions of pyrite, sulfate and water, and concentrations of major and trace elements demonstrate a geogenic source for arsenic linked to the dissolution of pyrite. We provide new tools to further study As at low concentrations where many processes may be masked. The observed negative correlation between $\delta^{34}S_{SO4}$ and [As] is interpreted as a Rayleigh-type sulfur-isotope fractionation during increasing pyrite dissolution. The observed positive correlation between $\delta^{18}O_{SO4}$ and As^{V}/As^{III} could help to retrieve initial redox conditions. A 3-year long monitoring at high-resolution demonstrated that drought conditions enhance pyrite dissolution whose degradation products are scavenged by recharge water. An increase in As in groundwater may result from droughts due to enhanced oxygen entry in the unsaturated zone. The 2003 European heatwave had a major effect.

1. Introduction

Many states lowered their limit for [As] in drinking water following the WHO guideline value of 10 μg/l [1] and costly actions are to be prepared. For water with arsenic concentration just above the limit, cost-effective solutions may not be treatment but mixing with low-arsenic concentration water. These solutions will be efficient only if they are dimensioned to the potential variations in As concentrations, and if the mechanisms able to increase [As] are evaluated. This requires that the origin of As in water is understood, and that the temporal evolution of [As] is assessed.

Smedley and Kinniburgh [1] presented a review of the source, behavior and distribution of arsenic in natural waters. Arsenic is mostly found in the environment as arsenite (As^{III}, reduced) and arsenate (As^{V}, oxidized). Its dominant forms are inorganic. Minerals commonly known to be a source for As in surface water and groundwater are arsenopyrite (FeAsS) and arsenian pyrite ($Fe(S, As)_2$). After mobilization from pyrite oxidative dissolution, As is often adsorbed on metal oxides and oxyhydroxides [2,3]. Arsenic can be mobilized from this secondary source either at pH above 7 or under reducing conditions [2,3].

Dissolution of pyrites is a complex process [4–7]. Mediated by bacteria or not, it produces sulfate with distinctive sulfur-isotope ratios used to determine its sulfide origin [8]. As pyrites may contain significant amounts of arsenic (see Section 2.1), sulfur isotopes may thus be used to link [As] measured in water with a potential pyrite source. Fractionation of ^{34}S and ^{32}S between sulfide and sulfate and fractionation of ^{18}O and ^{16}O between sulfate and water have been the focus of much attention, mainly due to acid

* Corresponding author at: CEA, DAM, DIF, F-91297 Arpajon, France. Tel.: +33 169265011.
E-mail addresses: Eric.Pili@cea.fr (E. Pili), Delphine.Tisserand@obs.ujf-grenoble.fr (D. Tisserand), Sarah.Bureau@obs.ujf-grenoble.fr (S. Bureau).

0304-3894/$ – see front matter © 2012 Elsevier B.V. All rights reserved.
http://dx.doi.org/10.1016/j.jhazmat.2012.07.004

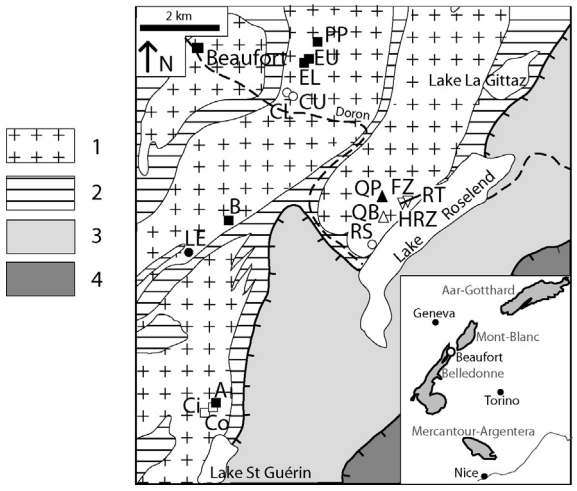

Fig. 1. Simplified geological setting of the Doron river catchment and location of the samples: (1) gneisses, micaschists, granites; (2) carboniferous sandstones, dolomite, quartzite, minor gypsum; (3) limestones and marls; (4) thrusted sedimentary units. Dashed line: Doron river. Squares: spring water captured and distributed. Circles: other springs. Triangle: surface water. Inverted triangles: groundwater. Black symbols: [As] > 10 μg/l. PP: Plan Perrier, EU: Echères (Upper), EL: Echères (Lower), CU: Cernix (Upper), CL: Cernix (Lower), B: Boudin, LE: Les Envers, A: Ami, Ci: Caponi inside tunnel, Co; Caponi outside tunnel, RS: Roselend spring, RT: Roselend tunnel, FZ: Fracture zone, HRZ: host rock zone, QP: quarry puddle, QB: quarry brook. Inset: the External Crystalline Massifs and the Beaufort area.

mine drainage issues [9–12]. Pyrite may be oxidized by dissolved molecular oxygen or ferric iron [4]. In the first case, oxygen in dissolved sulfate is contributed by O_2 and H_2O, in the second case, oxygen is contributed by H_2O only. A transition from one mode of dissolution to the other was observed during bacteria-mediated experiments [13]. Under certain limitations, $\delta^{18}O_{SO4}$ and $\delta^{18}O_{H2O}$ have the potential to decipher aerobic and anaerobic conditions or biotic and abiotic pathways [9,11,12,14].

Here, we report a study of arsenic in spring water distributed in the area of Beaufort, a town of <2500 inhabitants in the French Alps. Some springs have [As] > 10 μg/l. Once this was established by the Regional Health Agency, a monthly monitoring started in 2005. The origin of As in water was unknown. For this study, we sampled spring water known to have [As] exceeding the guideline. We also collected samples from groundwater and surface water nearby. From a series of measurements of major, minor and trace element concentrations, As speciations and S–O-isotope ratios, we propose a primary source for arsenic from pyrite and mechanisms leading to its mobility. The dynamics of pyrite dissolution was studied thanks to a long-term and high-resolution monitoring of [SO_4] and water flow rate. The archives of the town of Beaufort on [As] and spring water flow rates were analyzed for their seasonal and long-term evolutions. The risk situations likely to increase arsenic concentrations in the collected spring water are presented in order to help the resource management.

2. Materials, sampling and methods

2.1. Setting

The town of Beaufort is built along the Doron river. The Doron river catchment (Fig. 1) belongs to the External Crystalline Massifs of the French Alps, whose backbone is an Hercynian basement made of crystalline rocks (gneisses, micaschists and granites), partially overlaid by a sedimentary cover.

Although this has been mainly overlooked in scientific papers, newspaper articles and health authorities reveal that numerous localities are facing issues of arsenic in groundwater along the more than 600-km long arc defined by the External Crystalline Massifs in France, from the Mont Blanc-Beaufort massif (this study, and D. Chabert, pers. comm., 2011), the Belledonne massif (L. Charlet, pers. comm., 2011) and to the Mercantour massif [15]. The same problem is found in Switzerland near the border with Italy (Valais, Ticino, Grisons) following the same arc [2,16].

We studied and sampled 10 springs that were originally equipped for water collection by the local authority (Fig. 1). Three of them (Cernix (Upper and Lower) and Les Envers) were abandoned, respectively because of bacteriological problems and because of close proximity with a road. The Caponi spring is an important inflow of water through a large fracture in the Caponi tunnel, formerly used for mining copper and other metals mostly associated with iron sulfide minerals. Extensive iron precipitates are observed at this spring. Six springs are known to have [As] > 10 μg/l: Plan Perrier, Echères (Upper), Echères (Lower), Boudin, Les Envers and Ami. Four springs (Plan Perrier, Echères (Upper), Echères (Lower), Boudin) are monitored monthly for flow rate and [As] since August 2005 by the local authority. For Echères (Upper) and Echères (Lower), only the mean concentration value and the sum of the two flow rates are recorded. Before the start of the monthly As monitoring, 6 measurements were available over the period 1998–2002.

All the springs are located in the crystalline rock unit (Fig. 1). Most of these crystalline rocks contain iron sulfides (mostly pyrites, including arsenopyrite and arsenian pyrite) with whole rock [As] in the range 1–30 ppm (see Supplementary Table 1). In the crystalline rock unit near Lake Roselend (Fig. 1) is hosted the Roselend Natural Laboratory, a research facility devoted to the study of fluid-rock interactions [17,18] and used to collect mineral and additional water samples. There, a tunnel provided access to the heart of the fractured-rock unsaturated zone, at 55 m depth, where sampling sites provided access to dripwater samples. The end of the Roselend tunnel corresponds at the topographic surface with a large quarry (ca. 500 m × 150 m) where a perennial puddle (stagnant water, less than 80 cm deep) had developed. A large amount of biomass is degraded in water. As a result, abundant Mn oxides precipitates were locally observed in the tunnel since October 2005. Reducing conditions in the quarry puddle mobilize Mn. After percolating through some fractures, Mn precipitates once it finds again oxidizing conditions in few zones of the tunnel.

2.2. Sample collection and storage

In the Roselend tunnel, dripwater samples were collected from a fracture-dominated zone (FZ, at 120 m from tunnel entrance) and a matrix-dominated zone (HRZ, at 125 m from entrance) [17]. Additional samples were collected at various distances along the tunnel (at 57 m, 80 m, 100 m from entrance, respectively samples D57, D80 and D100) and surface water was collected at its entrance (D10, runoff water). Sample D80 was collected in a zone locally rich in pyrites. Minor Fe-oxide precipitates were locally observed in this zone. The Roselend quarry was used to collect surface water from its puddle and from the brook that flows from it. A nearby spring provided an additional sample. Samples were collected mostly in June 2011, after 1 week of heavy rain. Two samples from the quarry were collected and analyzed in April 2011 after 3 weeks of dry weather. Three water samples from the tunnel had been collected and analyzed in March and June 2004. The names, types of sample and dates of sampling are listed in Table 1. We also used [SO_4] measured from dripwater samples collected from the FZ sampling zone during a long-term (June 2002–June 2005) and high resolution (time step of 2–4 days) monitoring experiment described elsewhere [17]. The protocol for the collection of water samples, including the types and the preparation of the bottles, filtration, preservation and storage, is reported in the Supplementary Protocol.

Table 1
Water chemistry.

Sample	Type[a]	Date of sampling	pH	Eh (mV)	HCO_3 (mg/l)	CO_3 (mg/l)	SO_4 (mg/l)	Ca (mg/l)	Mg (mg/l)	Na (mg/l)	K (mg/l)	DOC (mg/l)
Plan Perrier	Sp	6/6/2011	7.9	491	70.2	–	14.7	21.1	3.0	1.2	0.5	0.41
Echères (Upper)	Sp	6/6/2011	8.1	465	107.7	<5	17.6	25.1	11.7	1.9	0.7	0.43
Echères (Lower)	Sp	6/6/2011	8.1	465	109.0	<5	16.2	25.1	7.5	1.5	0.7	0.45
Cernix (Upper)	Sp	6/6/2011	7.5	465	93.9	<5	40.8	36.9	6.8	2.5	1.0	5.52
Cernix (Lower)	Sp	6/6/2011	7.4	473	89.7	<5	77.0	48.7	8.4	3.0	1.0	36.3
Boudin	Sp	6/6/2011	7.2	458	57.2	<5	21.1	23.4	3.8	2.7	0.5	0.82
Les Envers	Sp	6/6/2011	8.4	440	112.4	7.4	19.2	38.1	5.7	1.7	0.6	0.85
Ami	Sp	6/7/2011	7.9	426	150.5	<5	42.9	49.7	8.5	0.9	0.4	0.36
Caponi outside	Sp	6/7/2011	7.6	374	183.0	<5	40.2	55.8	8.3	0.2	0.4	0.35
Caponi inside	Sp	6/7/2011	–	–	170.3	<5	39.7	53.9	7.9	2.2	0.6	0.48
Roselend Spring	Sp	6/7/2011	8.1	428	198.4	<5	97.0	75.9	12.6	1.3	5.8	2.53
Quarry Puddle	SW	4/15/2011	9.9	–	110.7	24.0	21.8	28.7	7.1	4.7	39.2	13.8
Quarry Puddle	SW	6/7/2011	9.0	400	117.1	<5	56.0	40.2	8.6	2.5	18.2	15.4
Quarry Brook	SW	4/15/2011	8.0	–	201.4	<5	184.6	92.4	20.1	1.5	10.2	7.33
D10	SW	6/7/2011	8.2	575	113.7	<5	19.8	35.0	5.5	1.4	0.4	1.61
D57	GW	6/15/2004	–	–	–	–	139.4	–	14.9	6.3	1.6	–
D80	GW	6/17/2004	–	–	–	–	955.7	272.8	92.6	5.2	2.8	–
D100	GW	3/2/2004	–	–	–	–	101.1	59.8	18.7	4.8	2.6	–
FZ-man1	GW	4/15/2011	–	–	–	–	45.0	–	–	–	–	5.88
FZ-auto	GW	4/15/2011	8.1	–	278.3	<5	41.9	84.4	17.6	6.0	9.4	189
FZ-auto	GW	5/21/2011	8.0	–	297.8	<5	42.3	90.2	18.1	6.1	13.0	5.16
HRZ-auto	GW	4/23/2011	7.8	–	222.7	<5	102.0	84.0	25.8	6.1	3.2	7.0
HRZ-auto	GW	5/25/2011	7.8	–	189.2	<5	97.3	74.3	23.5	5.6	2.4	11.4

Sample	Fe (μg/l)	Mn (μg/l)	As^{III} (μg/l)	DMA^V (μg/l)	MMA^V (μg/l)	As^V (μg/l)	As total[b] (μg/l)	As^V/As^{III}	$\delta^{34}S_{SO4}$ (‰CDT)	$\delta^{18}O_{SO4}$ (‰VSMOW)	$\delta^{18}O_{H2O}$ (‰VSMOW)
Plan Perrier	1.36	<0.02	<0.10	<0.04	<0.01	9.27	9.27	>93	7.44 ± 0.05	−4.56 ± 0.23	−12.53 ± 0.01
Echères (Upper)	1.81	<0.02	<0.10	<0.04	<0.01	6.12	6.12	>61	8.38 ± 0.05	−5.35 ± 0.18	−12.25 ± 0.01
Echères (Lower)	1.31	<0.02	<0.10	<0.04	<0.01	9.51	9.51	>95	7.52 ± 0.06	−6.17 ± 0.33	−12.14 ± 0.01
Cernix (Upper)	0.74	<0.02	<0.10	20.74	<0.01	6.62	6.62	>66	6.87 ± 0.01	0.44 ± 0.28	−12.06 ± 0.01
Cernix (Lower)	0.95	<0.02	<0.10	<0.04	<0.01	5.84	5.84	>58	10.67 ± 0.05	7.51 ± 0.22	−11.98 ± 0.01
Boudin	1.15	<0.02	<0.10	<0.04	<0.01	10.18	10.18	>101	4.94 ± 0.09	−3.13 ± 0.14	−12.02 ± 0.01
Les Envers	1.37	<0.02	0.21	<0.04	<0.01	8.07	8.28	38.4	6.51 ± 0.06	−1.54 ± 0.22	−12.17 ± 0.01
Ami	1.05	<0.02	<0.10	<0.04	<0.01	13.94	13.94	>139	2.75 ± 0.07	−10.18 ± 0.29	−12.55 ± 0.01
Caponi outside	2.57	17.10	0.32	<0.04	<0.01	2.86	3.19	8.9	1.85 ± 0.18	−8.59 ± 0.05	−12.59 ± 0.01
Caponi inside	3.78	29.64	0.29	<0.04	<0.01	2.25	2.54	7.8	2.12 ± 0.08	−8.73 ± 0.28	−12.58 ± 0.01
Roselend Spring	2.37	<0.02	<0.10	<0.04	<0.01	<0.15	<0.03	18.3	7.74 ± 0.33	−5.39 ± 0.29	−12.80 ± 0.01
Quarry Puddle	331.4	25.05	1.13	1.92	1.26	20.73	25.04	4.2	–	–	−12.28 ± 0.01
Quarry Puddle	151.1	38.32	1.24	<0.04	<0.01	5.15	6.39	1.7	7.14 ± 0.18	−7.65 ± 0.37	−9.27 ± 0.02
Quarry Brook	18.27	14.04	0.40	0.04	0.12	0.66	1.22	6.6	–	–	−14.32 ± 0.01
D10	1.10	<0.02	<0.10	<0.04	<0.01	<0.15	<0.03	–	1.09 ± 0.12	−8.28 ± 0.24	−12.87 ± 0.01
D57	–	–	–	–	–	–	14.85	–	−0.10 ± 0.30	−6.50 ± 0.30	−11.83 ± 0.02
D80	–	7.46	1.5	–	–	3.62	5.16	2.4	6.25 ± 0.30	−9.89 ± 0.30	−12.17 ± 0.02
D100	–	–	3.87	–	–	25.5	29.40	–	0.26 ± 0.30	−4.91 ± 0.30	−11.69 ± 0.02
FZ-man1	–	–	–	–	–	–	<0.03	–	9.09 ± 0.03	1.55 ± 0.30	−12.26 ± 0.02
FZ-auto	1.05	1012	<0.10	<0.04	<0.01	<0.15	<0.03	–	–	–	−12.26 ± 0.02
FZ-auto	0.91	927	<0.10	<0.04	<0.01	<0.15	<0.03	–	–	–	−12.20 ± 0.01
HRZ-auto	1.02	3.32	<0.10	<0.04	<0.01	<0.15	<0.03	–	–	–	−11.87 ± 0.02
HRZ-auto	0.91	1.17	–	–	–	–	<0.03	–	–	–	−12.09 ± 0.02

[a] Sp: spring water, SW: surface water, GW: ground water. b Sum of the As species determined by HPLC + ICP-MS or determination by ICP-MS.

From petrographical examination confirmed by chemical analyses (Supplementary Table 1), three types of pyrites were sampled inside the Roselend tunnel from fresh surfaces in two distinct settings (Table 2) in order to get an overview of the possible isotopic compositions of these minerals in the crystalline rock unit. Dripwater was collected in the same zones of the tunnel (D57, D80) for comparison of the isotopic compositions.

2.3. Sample analyses

Temperature, pH, redox potential and conductivity were measured during sampling using a WTW 340i multiparameter. Alkalinity was determined within 24 h using Gran titration. The determination of total dissolved As and Fe was performed by ICP-MS [19] with a precision better than 3%. Analyses of dissolved

Table 2
Sulfide minerals from the Roselend tunnel, their As content and sulfur isotopic compositions and the fractionation between sulfates dissolved in water and the mineral.

Sample	Type[a]	Setting	As content (ppm)	$\delta^{34}S_{mineral}$ (‰ VCDT)	$\varepsilon^{34}S_{sulfate-mineral}$ (‰ VCDT)
04R06a	Arsenopyrite (80 m)	cm-size cubes from 1-m thick quartz vein	19.6	8.25	−2.00
04R07a	Chalcopyrite (80 m)	cm-size cubes from 1-m thick quartz vein	4.20	7.80	−1.55
04R05a	Pyrite (57 m)	mm-size cubes from a micaschist	4.40	15.00	−15.10

[a] With indication of distance from tunnel entrance in meter.

arsenic species (As^{III}, monomethylarsenic MMA, dimethylarsenic DMA and As^{V}) were carried out using anion exchange chromatography column coupled to an ICP-MS [19]. The detection limits were 0.1 μg/l for As^{III}, 0.15 μg/l for As^{V}, 0.04 μg/l for DMA and 0.01 μg/l for MMA, with a precision better than 5%. For the monthly monitoring, arsenic was determined following standard method NF EN 26595 (silver diethyldithiocarbamate spectrometric method). Dissolved major anions (Cl, NO_3, SO_4, PO_4) and cations (Mg, Ca, Na, K) were determined by ion chromatography with a detection limit of 0.1 mg/l and a precision better than 5%. Ionic balances were calculated and accepted when better than 7%. DOC was determined using a Shimadzu VCSN analyzer with a detection limit of 0.3 mg/l and a precision better than 2.5%.

Dissolved sulfates were precipitated as $BaSO_4$ prior to oxygen and sulfur isotopes analysis with an elemental analyzer coupled with an isotope ratio mass spectrometer (IRMS) [20]. Determination of oxygen isotopes in water were analyzed by IRMS after standard CO_2 equilibration [21]. Isotope analyses are reported in per mil notation (‰) with reference to the Vienna Canyon Diablo Troilite standard (VCDT) for sulfur ($\delta^{34}S_{SO4}$) and to the Vienna Standard Mean Ocean Water (VSMOW) for oxygen ($\delta^{18}O_{SO4}$ and $\delta^{18}O_{H2O}$).

3. Results and discussion

The main features of water chemistry for all the water samples collected in this study are displayed in Table 1. $\delta^{34}S$ of pyrites are given in Table 2. Averaged flow rates and [As] as well as other descriptive parameters from the monthly monitoring are reported in Table 3 while the complete dataset is given in Supplementary Table 2.

3.1. Water geochemistry

Total arsenic concentrations span 2 orders of magnitude, ranging from <0.3 μg/l (detection limit) to nearly 30 μg/l (Tables 1 and 3). Total arsenic concentrations in springs go up to 14 μg/l (Ami) in water sampled for this study and up to 16 μg/l (Plan Perrier) in the monitored springs (2005–2011). Arsenic concentrations go up to 25 μg/l in surface water (Quarry Puddle) and up to 29 μg/l in groundwater (D100).

The geochemical processes responsible for the origin and the mobility of As may be masked when only looking at [As]. In surface water and spring water, and with a minor effect in groundwater due to longer residence times, dilution by rain water or by very low-As water contributions may greatly lower [As]. This is most probably the case in the quarry puddle. Also, a long-lasting rain has resulted in dilution of the sampled spring water. Indeed, our samples collected in early June 2011 after 1 week of heavy rain gave lower arsenic concentrations than samples collected 10 days after for monitoring by the local authority under dry weather conditions. Values are respectively 7.9 μg/l and 10.8 μg/l for Echères, and 9.3 μg/l and 13.3 μg/l for Plan Perrier (Supplementary Table 2 and Table 1), which corresponds to ca. 30% of dilution by rain water in both cases. Also, sorption of As onto Fe or Mn oxide precipitates and onto natural organic matter may strongly lower its concentration in water [3]. As shown in Table 1, relatively high concentrations in Fe and Mn (respectively in the ranges 2–4 μg/l and 17–30 μg/l) in water flowing from the Caponi tunnel are associated with low [As] ~ 3 μg/l. To a lesser extent, water samples from zone D80 in the Roselend tunnel are associated with moderate [As] relatively to the local abundance of arsenopyrite and minor Fe oxide precipitates are observed. High DOC and Mn contents, associated with Mn oxide precipitates, go with low [As] in the FZ zone of the Roselend tunnel. More generally, DOC > 1 mg/l goes with As < 0.3 μg/l.

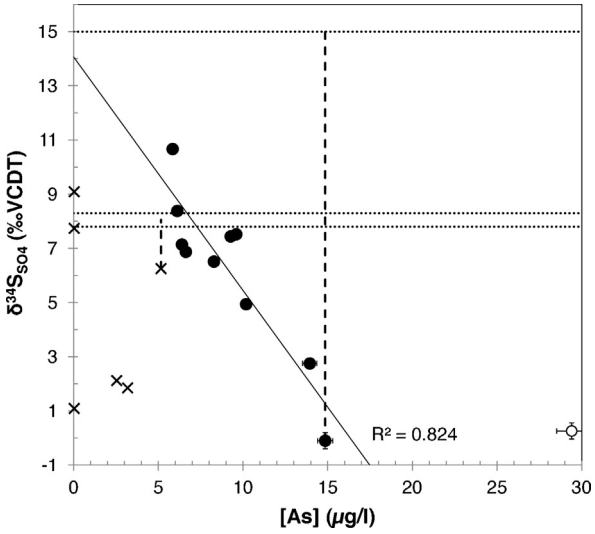

Fig. 2. Plot of the $\delta^{34}S$ value of dissolved sulfate vs. [As]. Crosses are samples collected in zones where precipitates of Fe or Mn oxides are observed, which is suspected to lower the arsenic concentrations. $\delta^{34}S_{SO4}$ correlates negatively with [As]. The regression line is calculated with the black dots. Sample D100 (open circle) is considered an outlier. Dotted lines: $\delta^{34}S$ of pyrites. Dashed lines: fractionation between dissolved sulfate and pyrites.

Exceptions are the quarry puddle due to its reducing conditions (Mn solubility, see Section 2.1) and the Cernix springs known to be contaminated by fecal matter.

Among all samples, As^{V} is the major arsenic species and As^{III} is rarely detected. The expected reducing conditions in the quarry puddle and brook are associated with As^{V}/As^{III} ratios from 2 to 7, while samples of water flowing through rocks rich in sulfide minerals in the Caponi tunnel and at zone D80 in the Roselend tunnel have As^{V}/As^{III} ratios from 2 to 9. As^{V}/As^{III} ratios in spring water are 18 (Roselend Spring) and 38 (Les Envers). Organic species of arsenic, MMA and DMA were only detected in organic-rich water from the quarry (puddle and brook). In a Pourbaix diagram (not shown), all the pH and Eh values indicate conditions where As is in the form $HAsO_4^{2-}$ (As^{V}). This discrepancy with measured As^{III} comes from the fast equilibration with oxidizing conditions for water pH and Eh while arsenic species equilibrate more slowly [1]. Arsenic speciation thus keeps the memory of water–mineral interactions at depth. This also confirms that As originates in a more reducing environment and at a lower pH than measured when water is sampled.

If arsenic in water originates from the dissolution of iron sulfide minerals, one may expect to observe correlations between the concentrations in As, Fe or SO_4. None is observed, consistently with the fact that As mobilized from the oxidation of pyrite is often trapped on secondary iron oxides [1,22]. Therefore the origin of As from pyrite is lost when looking at the major element geochemistry of water. This is one of the reasons why sulfur and oxygen isotopes from dissolved sulfate should be used.

3.2. Sulfur isotopes

$\delta^{34}S_{SO4}$ values for spring water, surface water and groundwater in the area of Beaufort range from −0.1‰ to +11‰ (Table 1). Most of the $\delta^{34}S_{SO4}$ values correlate negatively with total [As] (Fig. 2, $r^2 = 0.824$). Exceptions are samples collected in zones where precipitates of Fe or Mn oxides are observed, which lowers [As]. One sample (D100, Table 1) with a high [As] may be considered as an outlier for an unknown reason and has been omitted in the regression line, although this does not change the general trend.

Table 3
Descriptive parameters of flow rates and [As] from three springs monitored monthly from August 2005 to August 2011.[a]

Month	Flow rate					Arsenic				
	Monthly averaged flow rate (l/s)	Standard deviation (l/s)	Min. flow rate (l/s)	Max. flow rate (l/s)	Number of data	Monthly averaged As concentration (μg/l)	Standard deviation (μg/l)	Min. [As] (μg/l)	Max. [As] (μg/l)	Number of data
Echères										
Jan	8.5	2.2	5.5	11.1	5	10.0	1.0	8.6	11.6	6
Feb	8.1	1.8	5.5	10.4	6	–	–	–	–	0
Mar	9.8	6.4	5.6	20.9	5	10.9	1.7	9.2	12.8	6
Apr	16.4	7.9	11.1	31.7	6	–	–	–	–	0
May	22.6	9.3	10.4	36.5	5	10.8	1.0	9.9	12.5	6
Jun	31.6	12.8	12.1	42.5	6	10.1	0.6	9.2	10.8	6
Jul	20.6	7.5	13.0	30.2	5	10.8	0.6	10.0	11.6	5
Aug	12.7	3.8	9.2	17.8	6	10.1	1.3	8.5	12.2	6
Sep	11.5	3.2	8.0	16.9	6	9.4	0.8	8.8	10.3	3
Oct	9.9	2.7	6.5	13.7	6	10.3	1.0	8.6	11.3	6
Nov	7.1	1.2	5.7	8.3	4	10.6	1.2	9.2	12.3	6
Dec	10.3	3.6	8.0	15.7	4	11.6	1.3	9.7	13.6	6
Plan Perrier										
Jan	7.9	2.6	5.1	12.0	5	–	–	–	–	0
Feb	7.4	1.6	5.0	8.7	6	–	–	–	–	0
Mar	12.3	8.3	4.9	20.8	4	13.4	2.2	10.5	16.1	5
Apr	13.6	6.7	8.8	25.0	5	–	–	–	–	0
May	17.1	9.8	6.7	32.4	5	12.0	1.9	9.7	14.9	6
Jun	16.4	9.0	8.8	29.5	5	11.4	2.7	9.5	13.3	2
Jul	17.0	7.8	9.2	30.0	5	–	–	–	–	0
Aug	11.6	4.4	7.9	20.0	7	12.9	2.0	10.9	15.1	4
Sep	10.3	2.3	6.7	13.6	6	11.2	1.7	10.0	12.4	2
Oct	8.3	1.7	5.6	10.0	6	10.4	–	–	–	1
Nov	6.2	0.9	4.9	7.0	4	13.6	2.5	11.8	15.3	2
Dec	10.0	3.5	6.9	14.7	4	12.9	1.7	11.2	15.6	6
Boudin										
Jan	1.4	0.6	0.7	2.5	6	–	–	–	–	0
Feb	1.1	0.3	0.7	1.5	6	–	–	–	–	0
Mar	1.5	1.1	0.9	3.8	6	12.4	1.8	10.3	14.2	4
Apr	2.4	1.8	1.1	6.1	6	–	–	–	–	0
May	1.6	0.4	1.0	2.1	6	12.5	0.6	11.9	13.1	5
Jun	1.8	0.4	1.3	2.5	6	15.0	–	–	–	1
Jul	1.6	0.3	1.4	1.9	6	–	–	–	–	0
Aug	1.3	0.4	0.7	1.7	7	11.3	1.6	9.3	13.3	6
Sep	1.3	0.5	0.9	2.1	6	11.0	1.4	10.0	12.0	2
Oct	1.1	0.4	0.8	1.8	6	10.0	0.6	9.6	10.4	2
Nov	0.9	0.3	0.7	1.5	6	10.4	0.8	9.8	10.9	2
Dec	1.5	1.0	0.7	3.2	6	13.5	1.9	11.2	15.8	6

[a] Complete data set is given in Supplementary table* 1.

The relationship between [As] and $\delta^{34}S_{SO4}$ can be understood as follows. Both As and SO_4 come from pyrite dissolution. Higher As concentrations in water mean either dissolution of pyrite containing higher amounts of As (Hypothesis #1) or higher amounts of dissolved pyrite (Hypothesis #2). Because SO_4 comes from pyrite dissolution, $\delta^{34}S_{SO4}$ has to be compared with $\delta^{34}S_{mineral}$ of the parent pyrite. The $\delta^{34}S_{mineral}$ values of 3 pyrites thought to be representative of the study area are 7.8‰, 8.25‰, and 15‰ (Table 2). The production of SO_4 from pyrite is known to be associated with a small fractionation of the sulfur-isotopes (hereafter referred as $\varepsilon^{34}s_{sulfate-mineral}$), typically between −1.8‰ and +0.8‰ [11,12]. The oxidation of chalcopyrite by Fe(III) is associated with $\varepsilon^{34}s_{sulfate-mineral}$ of -4.0 ± 0.4‰ (biologically mediated) and -3.7 ± 1.2‰ (abiotic), while oxidation by O_2 leads to $\varepsilon^{34}s_{sulfate-mineral}$ of -1.5 ± 0.2‰ (biologically mediated) and -0.5 ± 0.7‰ (abiotic) [23]. Following Hypothesis #1, the observed negative correlation between $\delta^{34}S_{SO4}$ and [As] in water should be associated with progressively decreasing $\delta^{34}S_{mineral}$ for pyrites containing increasing amounts of As. We are not aware of any study reporting such a relation between $\delta^{34}S_{mineral}$ and As content in pyrite. In addition, the apparent $\varepsilon^{34}s_{sulfate-mineral}$ can be calculated from the isotope composition of dripwater collected from the zones where pyrites are sampled (Table 2, Fig. 2). We obtain small values as expected from literature data [11,12,23], with $\varepsilon^{34}s_{sulfate-mineral} = -2.0$‰ for arsenopyrite and −1.6‰ for chalcopyrite, assuming the same water (sample D80) has been in contact with the two types of sulfide. However, a very large apparent fractionation factor of −15.1‰ is calculated for our pyrite and water (D57) samples. This leads to favor Hypothesis #2, where the observed negative correlation between $\delta^{34}S_{SO4}$ and [As] in water is associated with increasing pyrite dissolution. The apparent $\varepsilon^{34}s_{sulfate-mineral}$ progressively increases due to cumulative fractionation at each step of dissolution. This suggests a sulfur-isotope fractionation process during the dissolution of As-bearing pyrite similar to a Rayleigh model [24] where sulfate is assumed to form in isotopic equilibrium with the parent pyrite and to be removed immediately. With such a model, small fractionation factors as experimentally measured [11,12] may thus account for large apparent fractionations. Alternatively, or in addition, successive oxidations of intermediate sulfoxy species [5,7,11,25] may be the elementary steps responsible for cumulated fractionations. In this view, the variety of $\delta^{34}S$ values of the source pyrites may not be the main contribution to the variety of $\delta^{34}S_{SO4}$ values. If it proves to be generalized, this relation between $\delta^{34}S_{SO4}$ and [As] could be used to retrieve [As] that should be observed in the absence of secondary trapping of As. This may help to determine a baseline in case of any natural or anthropogenic event that might modify this secondary reservoir of As known to be versatile [1–3].

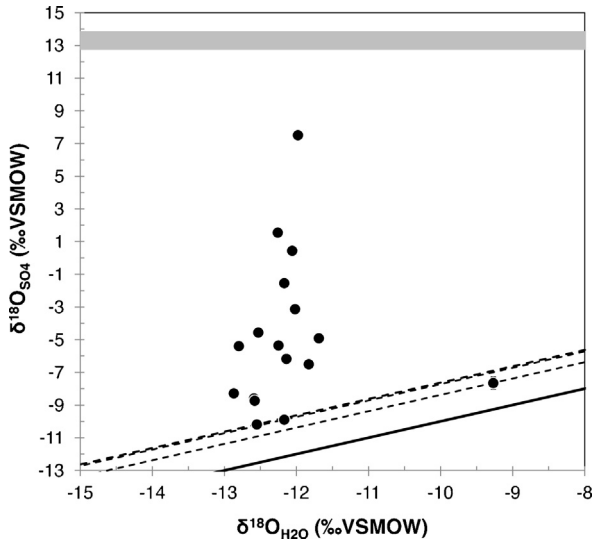

Fig. 3. Plot of the $\delta^{18}O$ value of dissolved sulfate vs. the $\delta^{18}O$ value of water. The solid line represents zero fractionation ($\delta^{18}O_{SO4} = \delta^{18}O_{H2O}$), the three dashed lines represent the anaerobic condition end-member constructed for three entitled samples (see Section 3.3). The grey zone represent the aerobic condition end-member. $\delta^{18}O_{SO4}$ values increase with an increasing amount of O_2 participating in pyrite dissolution.

3.3. Oxygen isotopes

Numerous literature data show that oxygen in sulfate is mostly incorporated from water [11,12]. The higher the $\delta^{18}O_{SO4}$, the lower the water-derived oxygen proportion. The plot $\delta^{18}O_{SO4}$ vs. $\delta^{18}O_{H2O}$ (Fig. 3) may be used cautiously to estimate if conditions were aerobic or anaerobic during pyrite dissolution. $\delta^{18}O_{SO4}$ values in our samples span a large range from −10‰ to +7.5‰ (Fig. 3), while $\delta^{18}O_{H2O}$ values are mostly around −12.3‰ similar to the average local meteoric water and groundwater [18]. Water from the quarry puddle has a markedly different isotopic composition ($\delta^{18}O_{H2O}$ = −9.27‰) because it results from a direct collection and mixing of precipitations whose monthly averaged $\delta^{18}O_{H2O}$ vary from −6‰ to −19‰, with a monthly averaged value for June at

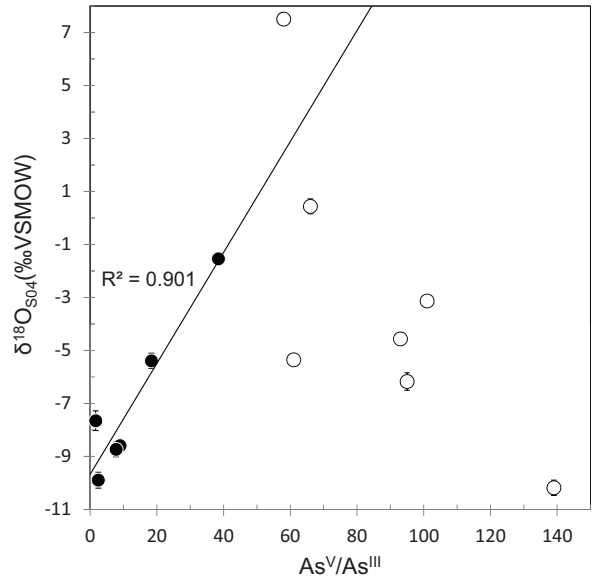

Fig. 4. Plot of the $\delta^{18}O$ value of dissolved sulfate vs. the As^V/As^{III} ratio. Dots are samples with measured amounts of As^{III} and As^V. Open symbols are samples with As^{III} < 0.1 μg/l (detection limit).

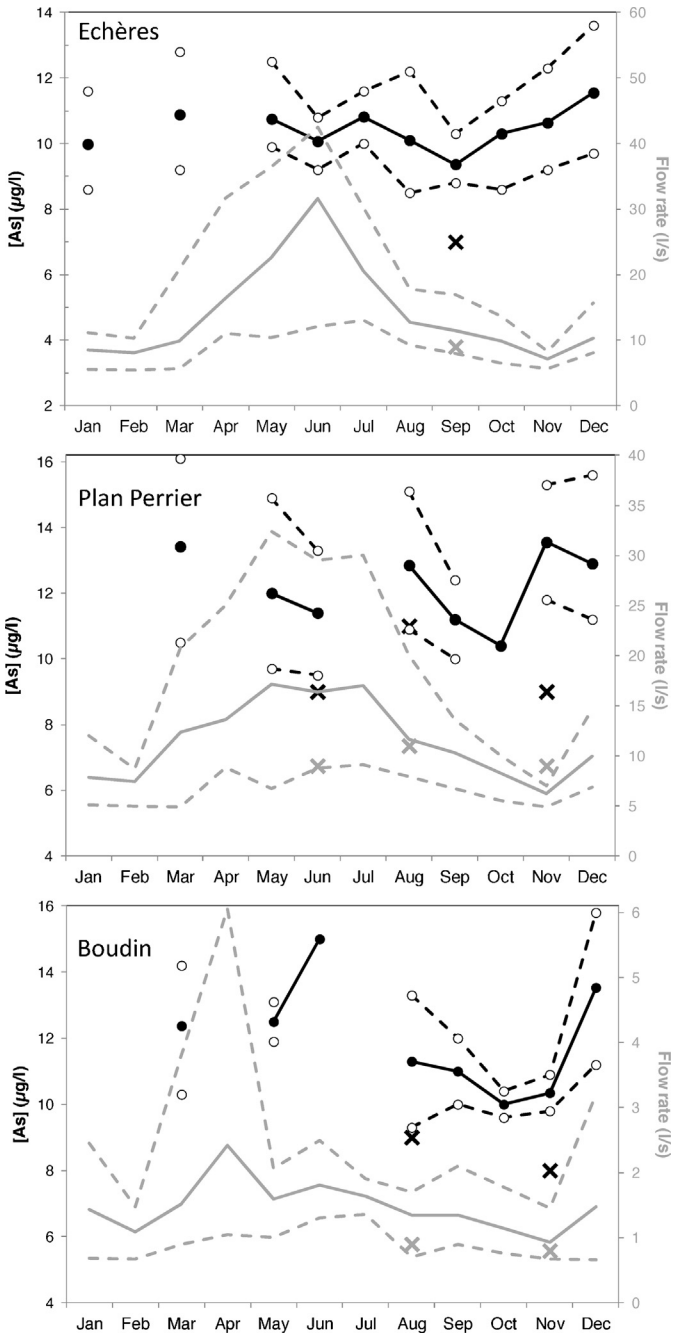

Fig. 5. Temporal evolution of monthly averaged [As] (black) and flow rates (grey) for the three monitored springs. Averages calculated from August 2005 to August 2011 (Table 3). Dashed lines and open symbols are min–max values. Crosses represent values measured before 2005.

−7.6‰ [18,26]. Evaporation may also be responsible for an increase in $\delta^{18}O_{H2O}$.

The large range in the $\delta^{18}O_{SO4}$ values (Fig. 3) reflects variable conditions from anaerobic to aerobic for the dissolution of pyrite and the production of arsenic. The measured $\delta^{18}O_{SO4}$ values do not correlate with [As]. This may be related with our limited sample set compared to a complete hydrological year. It may also be related to the complex redox processes controlling As mobility [1–3]. If $\delta^{18}O_{SO4}$ is controlled by the type of dissolution, aerobic vs. anaerobic, these conditions should also be recorded in the measured As^V/As^{III} ratios. Indeed, the $\delta^{18}O_{SO4}$ values are correlated with the As^V/As^{III} ratios (Fig. 4). However, this correlation is lost for water samples with [As^{III}] < 0.1 μg/l (detection limit). This suggests that

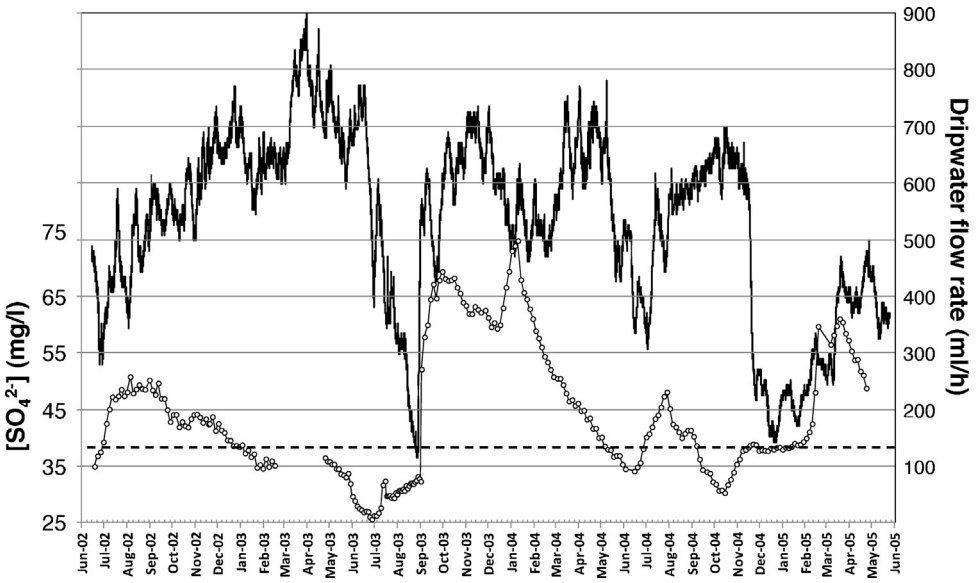

Fig. 6. Temporal evolution of [SO_4] (open circles) and flow rate of water dripping from the FZ (fracture-dominated) zone in the Roselend tunnel. The dashed line is the average [SO_4] calculated from June 2002 to August 2003. Summer and winter drought conditions are associated with increases in [SO_4].

$\delta^{18}O_{SO4}$ values keep memory of the initial conditions that mobilized As from pyrite dissolution, while the As^V/As^{III} ratios are losing this memory below a threshold [As^{III}].

A precise quantification of the water-derived oxygen proportion in sulfate requires that values of the fractionation factors for oxygen between sulfate and water ($\varepsilon_{SO4-H2O}$) and between sulfate and molecular oxygen (ε_{SO4-O2}) are known [11], following the equation [12]:

$$\delta^{18}O_{SO4} = X(\delta^{18}O_{H2O} + \varepsilon_{SO4-H2O}) + (1-X)(\delta^{18}O_{O2} + \varepsilon_{SO4-O2}), \quad (1)$$

where X and $(1-X)$ are the relative proportions of water-derived and molecular oxygen in sulfate, respectively. From experimental data, the slope of a linear regression of $\delta^{18}O_{SO4}$ vs. $\delta^{18}O_{H2O}$ values equals the water-derived oxygen proportion in sulfate. These lines cannot be traced from our field data because $\delta^{18}O_{H2O}$ values do not vary much and our samples do not represent the same conditions in terms of source pyrite, chemistry and isotopic composition of water, and residence time. Assuming that the measured low $\delta^{18}O_{SO4}$ values correspond with the oxidation of pyrite without O_2 ($X \rightarrow 1$), we may tentatively estimate $\varepsilon_{SO4-H2O} = \delta^{18}O_{SO4} - \delta^{18}O_{H2O}$. This is a measurement of the minimum distance between the line $\delta^{18}O_{SO4} = \delta^{18}O_{H2O}$ (zero-fractionation line) and the nearest samples. As shown in Fig. 3, three samples are entitled to this task. All three show evidence for strong reducing conditions (see Section 3.1). We obtained $\varepsilon_{SO4-H2O}$ values of 1.6‰, 2.3‰ and 2.4‰, for samples Quarry Puddle, D80 and Ami respectively (Table 1 and Fig. 3). A range in $\varepsilon_{SO4-H2O}$ values from 0.5‰ to 3.1‰ was determined experimentally [12,27]. Literature data indicate $\varepsilon_{SO4-O2} = -10.2 \pm 0.5$‰ [11]. With this range of fractionation factor and $\delta^{18}O_{O2} = 23.5$‰ [28], an indicative upper limit for the aerobic conditions can be drawn in Fig. 3. $\delta^{18}O_{SO4}$ from our samples cover a large range between aerobic and anaerobic conditions. As for the biotic/abiotic conditions, there is a debate in the literature whether this can be estimated from the $\delta^{18}O_{SO4}$ values [14,29,30] or not [11,12].

3.4. Temporal evolution

The evolution of monthly averaged [As] and flow rates for the three monitored springs over the years 2005–2011 is illustrated in Fig. 5. These data are partial because it is difficult for a small town to maintain such a monitoring. Flow rates show a peak between April and June, due to recharge by snow melting and rainfall. Low-flow is observed in November. No clear tendency can be found regarding the relation between flow rates and [As], except a slight change (decrease then increase) in [As] in September or October when flow rate is decreasing. The lack of [As] measurements on certain months and the monthly resolution are two disadvantages in this approach. Nevertheless, our 2005–2011 monthly averages may be use for comparison with some rare older values from year 1998–2002 (Fig. 5). Flow rates measured in June 1998, August 2002, September 1999 and November 2001 plot in the same min–max range as the 2005–2011 data. With regard to [As], all but one sample plot below the minimum values, three samples plot within 1σ (standard deviation) from the mean value, 1 sample plots within 2σ, and 2 samples plot within 3σ (Table 3, Supplementary Table 2). Although this statistical description is hampered by the small number of data, there are some indications that [As] in years 1998–2002 may have been lower than in years 2005–2011.

For a better understanding of the temporal evolution of concentrations, a higher-resolution is needed. The monitoring of [SO_4] and flow rates from the FZ sampling zone of the Roselend tunnel is presented in Fig. 6 for the period June 2002–June 2005. High water flow rates measured in this zone around 700 ml/h are known to indicate that rocks are saturated [17]. At first order, a yearly cycle is observed, with low [SO_4] in winter and spring when flow rate is high (dilution) and high [SO_4] in summer when flow rate is low (concentration). The mean [SO_4] over the period June 2002–August 2003 is 38 mg/l and it is consistent with the mean concentration for the period May 2004–February 2005. A severe drought occurred as a result of the 2003 European summer heatwave. Water recharge after drought was immediately followed by a large increase in [SO_4] that lasted about 5 months. From July 2003 to January 2004. [SO_4] is multiplied by a factor of 3. Severe drought conditions were also observed in winter 2004–2005 with a smaller increase in [SO_4]. Sulfate production is needed in order to increase its concentration. During drought conditions, air replaces water in the rock porosity. Our monitoring indicates that pyrite dissolution is enhanced in these conditions, and that the produced sulfate is flushed on recharge. The change from a water-saturated environment to an aerated one may have resulted in the change from chemical oxidation pathways to microbially mediated pathways as also suggested by Taylor et al. [29].

The fact that the summer drought had more effect than the winter one may be due to a temperature effect, an effect of the snow cover on gas exchange or to the availability of nutrients. Although not measured at that time, arsenic that comes with pyrite dissolution might well have had the same increase in concentration. The suspected increase in arsenic concentrations between years 1998–2002 and years 2005–2011 (Fig. 5) could have resulted from an enhanced As production promoted by an enhanced dissolution of pyrites due to air entry in the unsaturated zone during the droughts of summer 2003 and winter 2004–2005 (Fig. 6). Similarly, extensive pumping is suggested to promote atmospheric oxygen entry into aquifers, altering redox conditions, and increasing the rate of As release from sulfide oxidation into groundwater [31].

4. Conclusion

We provided new tools to further study As at low concentrations where many processes may be masked. The negative correlation between $\delta^{34}S_{SO4}$ and [As] is here interpreted as a Rayleigh-type sulfur-isotope fractionation during increasing pyrite dissolution. Laboratory experiments are necessary to confirm this result. The alternative hypothesis would require progressively decreasing $\delta^{34}S_{mineral}$ for cogenetic pyrites containing increasing amounts of As. This is not yet reported in the literature and could be tested from experiments or measurements from natural examples. As^V/As^{III} keeps better memory of the redox conditions than Eh. The positive correlation observed between $\delta^{18}O_{SO4}$ and As^V/As^{III} confirms that $\delta^{18}O_{SO4}$ is controlled by the type of dissolution, aerobic vs. anaerobic. A $\delta^{18}O_{SO4}$ vs. As^V/As^{III} plot could prove to be more meaningful than a classical $\delta^{18}O_{SO4}$ vs. $\delta^{18}O_{H2O}$ one, especially when $\delta^{18}O_{H2O}$ values do not vary much. It could help to retrieve initial redox conditions. Long-term and high-resolution monitoring demonstrated that drought conditions enhance pyrite dissolution whose degradation products are scavenged by recharge water. The 2003 European heatwave had a major effect. Among the potential mechanisms able to increase the rate of As release in groundwater, drought conditions must be taken into account. It mainly acts through oxygen entry in the unsaturated zone. Other human actions with similar effects should be avoided, such as an increase in groundwater pumping or a multiplication of the number of collection points for spring water that would otherwise be re-infiltrated. In the studied alpine catchment, As concentrations in groundwater increased between 1998 and 2005 most probably after the droughts of summer 2003 and of winter 2004–2005.

Acknowledgements

This work was funded by CEA. We thank the City of Beaufort sur Doron, particularly Annick Cressens, Mathias Sallansonnet, and Germain Wiki, for facilitating access to the springs for sampling and for sharing the 1998–2011 monitoring data. The help of Anne-Marie Boullier (ISTerre Grenoble) and Jimmy Bertrand (deceased) for understanding the geology, petrology and mineralogy of the area, and for the drawing of the geological map, is greatly acknowledged. Corinne Casiot, Sandra Van Exter, Sophie Delpoux, and Rémi Freydier (Hydrosciences Montpellier) are thanked for the As concentration and speciation measurements. Christian France-Lanord, Caroline Guillemette and Thomas Rigaudier (CRPG Nancy) are thanked for the isotope analyses. Sophie Guillon is thanked for her help during sampling. Fruitful discussion with Laurent Charlet is appreciated.

Appendix A. Supplementary data

Supplementary data associated with this article can be found, in the online version, at http://dx.doi.org/10.1016/j.jhazmat.2012.07.004.

References

[1] P.L. Smedley, D.G. Kinniburgh, A review of the source, behaviour and distribution of arsenic in natural waters, Appl. Geochem. 17 (2002) 517–568.
[2] H.R. Pfeifer, A. Gueye-Girardet, D. Reymond, C. Schlegel, E. Temgoua, D.L. Hesterberg, J.W.Q. Chou, Dispersion of natural arsenic in the Malcantone watershed, Southern Switzerland: field evidence for repeated sorption–desorption and oxidation–reduction processes, Geoderma 122 (2004) 205–234.
[3] S.L. Wang, C.N. Mulligan, Natural attenuation processes for remediation of arsenic contaminated soils and groundwater, J. Hazard. Mater. 138 (2006) 459–470.
[4] P.C. Singer, W. Stumm, Acidic mine drainage: the rate-determining step, Science 167 (1970) 1121–1123.
[5] C.O. Moses, D.K. Nordstrom, J.S. Herman, A.L. Mills, Aqueous pyrite oxidation by dissolved-oxygen and by ferric iron, Geochim. Cosmochim. Acta 51 (1987) 1561–1571.
[6] J.D. Rimstidt, D.J. Vaughan, Pyrite oxidation: a state-of-the-art assessment of the reaction mechanism, Geochim. Cosmochim. Acta 67 (2003) 873–880.
[7] M. Descostes, E. Tevissen, Definition of an equilibration protocol for batch experiments on Callovo-Oxfordian argillite, Phys. Chem. Earth Parts A/B/C 29 (2004) 79–90.
[8] D.E. Canfield, Biogeochemistry of sulfur isotopes, in: J.W. Valley, D.R. Cole (Eds.), Stable Isotope Geochemistry, Mineral. Soc. Am., Washington, 2001, pp. 607–636.
[9] B.E. Taylor, M.C. Wheeler, D.K. Nordstrom, Isotope composition of sulfate in acid-mine drainage as measure of bacterial oxidation, Nature 308 (1984) 538–541.
[10] R.O. van Everdingen, H.R. Krouse, Isotope composition of sulphates generated by bacterial and abiological oxidation, Nature 315 (1985) 395–396.
[11] N. Balci, W.C. Shanks Iii, B. Mayer, K.W. Mandernack, Oxygen and sulfur isotope systematics of sulfate produced by bacterial and abiotic oxidation of pyrite, Geochim. Cosmochim. Acta 71 (2007) 3796–3811.
[12] C. Heidel, M. Tichomirowa, The isotopic composition of sulfate from anaerobic and low oxygen pyrite oxidation experiments with ferric iron – new insights into oxidation mechanisms, Chem. Geol. 281 (2011) 305–316.
[13] B. Brunner, J.-Y. Yu, R.E. Mielke, J.A. MacAskill, S. Madzunkov, T.J. McGenity, M. Coleman, Different isotope and chemical patterns of pyrite oxidation related to lag and exponential growth phases of *Acidithiobacillus ferrooxidans* reveal a microbial growth strategy, Earth Planet. Sci. Lett. 270 (2008) 63–72.
[14] D.R. Van Stempvoort, H.R. Krouse, Controls of $\delta^{18}O$ in sulfate: review of experimental data and application to specific environments, in: J.L. Jambor, D.W. Blowes, A.I.M. Ritchie (Eds.), Environmental Aspects of Mine Wastes, Mineral. Assoc. Can., 1994, pp. 447–479.
[15] G. Feraud, C. Potot, J.F. Fabretti, Y. Guglielmi, M. Fiquet, V. Barci, P.C. Maria, Trace elements as geochemical markers for surface waters and groundwaters of the Var River catchment (Alpes Maritimes, France), C. R. Chim. 12 (2009) 922–932.
[16] H.-R. Pfeifer, J. Zobrist, Arsenic in drinking water – also a problem in Switzerland? EAWAG News 53 (2002) 15–17.
[17] E. Pili, S. Bureau, F. Perrier, D. Patriarche, L. Charlet, P.M. Adler, P. Richon, Reactive transport and residence times in unsaturated fractured rocks from field-scale experiments, in: M. Barnett, O.D.B. Kent (Eds.), Dev. Earth Environ. Sci., Elsevier Science B.V., 2008, pp. 441–468.
[18] E. Pili, F. Perrier, P. Richon, Dual porosity mechanism for transient groundwater and gas anomalies induced by external forcing, Earth Planet. Sci. Lett. 227 (2004) 473–480.
[19] O. Bruneel, A. Volant, S. Gallien, B. Chaumande, C. Casiot, C. Carapito, A. Bardil, G. Morin, G.E. Brown, C.J. Personne, D. Le Paslier, C. Schaeffer, A. Van Dorsselaer, P.N. Bertin, F. Elbaz-Poulichet, F. Arsene-Ploetze, Characterization of the active bacterial community involved in natural attenuation processes in arsenic-rich creek sediments, Microbial Ecol. 61 (2011) 793–810.
[20] A. Brenot, J. Carignan, C. France-Lanord, M. Benoît, Geological and land use control on [delta]^{34}S and [delta]^{18}O of river dissolved sulfate: the Moselle river basin, France, Chem. Geol. 244 (2007) 25–41.
[21] S. Epstein, T.K. Mayeda, Variations of ^{18}O content of waters from natural sources, Geochim. Cosmochim. Acta 4 (1953) 213–224.
[22] H.-R. Pfeifer, A. Häussermann, J.-C. Lavanchy, W. Halter, Distribution and behavior of arsenic in soils and waters in the vicinity of the former gold-arsenic mine of Salanfe, Western Switzerland, J. Geochem. Explor. 93 (2007) 121–134.
[23] R.S. Thurston, K.W. Mandernack, W.C. Shanks, Laboratory chalcopyrite oxidation by *Acidithiobacillus ferrooxidans*: oxygen and sulfur isotope fractionation, Chem. Geol. 269 (2010) 252–261.
[24] J. Hoefs, Stable Isotope Geochemistry, 3rd ed., Springer-Verlag, 1987.
[25] A. Schippers, P.G. Jozsa, W. Sand, Sulfur chemistry in bacterial leaching of pyrite, Appl. Environ. Microbiol. 62 (1996) 3424–3431.

[26] IAEA/WMO, Global Network for Isotopes in Precipitation. The GNIP Database, IAEA/WMO, 2011.
[27] A. Mazumdar, T. Goldberg, H. Strauss, Abiotic oxidation of pyrite by Fe(III) in acidic media and its implications for sulfur isotope measurements of lattice-bound sulfate in sediments, Chem. Geol. 253 (2008) 30–37.
[28] P. Kroopnick, H. Craig, Oxygen isotope fractionation in dissolved-oxygen in deep-sea, Earth Planet. Sci. Lett. 32 (1976) 375–388.
[29] B.E. Taylor, M.C. Wheeler, D.K. Nordstrom, Stable isotope geochemistry of acid-mine drainage – experimental oxidation of pyrite, Geochim. Cosmochim. Acta 48 (1984) 2669–2678.
[30] G. Lipfert, W.C. Sidle, A.S. Reeve, R.A. Ayuso, A.J. Boyce, High arsenic concentrations and enriched sulfur and oxygen isotopes in a fractured-bedrock ground-water system, Chem. Geol. 242 (2007) 385–399.
[31] Y.H. Kao, S.W. Wang, C.W. Liu, P.L. Wang, C.H. Wang, S.K. Maji, Biogeochemical cycling of arsenic in coastal salinized aquifers: evidence from sulfur isotope study, Sci. Total Environ. 409 (2011) 4818–4830.